

Search for high-energy neutrinos from local superbubbles with the ANTARES telescope

The ANTARES Collaboration^{‡*}

[‡] full author list at *PoS(ICRC2019)1177*

E-mail: luigi.fusco@apc.in2p3.fr

Some peculiarities of our Galactic neighbourhood could be responsible of significant features in the all-sky spectra of cosmic neutrinos, in particular in the tens-of-TeV energy range. The ANTARES neutrino telescope is most sensitive to neutrinos in this energy range and can test possible emissions over large parts of the sky.

Stellar winds and Supernovae can create regions of low matter density; the cumulative effect of many, close-by, active stars is the formation of “bubbles” with a rather low-density environment and “walls” at their borders where matter density and magnetic fields are enhanced. The Loop1 structure dominates the sky at radio wavelengths and is allegedly produced by the interaction of the Local Bubble, where our Solar System resides, and the bubble inflated by stellar activity in the Cen-Sco association, a group of large active stars close to us. Some models predict an increased cosmic ray interaction rate at the surface of contact between the two bubbles, which could be contributing to the overall cosmic neutrino signal.

A search for neutrinos from the Loop1 region has been carried out using data collected by the ANTARES neutrino telescope over 11 years of data acquisition. Track-like upward-going events are considered, the event selection being optimised to achieve the best sensitivity to a large-scale emission of neutrinos. The results of this analysis are presented in this contribution. A non-significant excess of events is observed from the signal region when compared to the estimated background.

Corresponding author: Luigi Antonio Fusco^{†1}

¹ APC, Univ Paris Diderot, CNRS/IN2P3, CEA/Irfu, Obs de Paris, Sorbonne Paris Cité, France

*36th International Cosmic Ray Conference -ICRC2019-
July 24th - August 1st, 2019
Madison, WI, U.S.A.*

*for collaboration list see also <http://antares.in2p3.fr/Collaboration/index2.html>

[†]Speaker.

1. Introduction

Neutrino astronomy aims at detecting the sources of high-energy cosmic neutrinos, so that the production and acceleration mechanisms of high-energy Cosmic Rays can be understood. The ANTARES neutrino telescope, located in the Mediterranean sea 40 km off-shore the coasts of Southern France, has been taking data since 2007 and has collected a large sample of neutrino candidates, used in various searches for cosmic neutrinos [1].

Data collected by the IceCube Neutrino Observatory have provided highly-significant observations of the existence of a diffuse cosmic neutrino flux [2, 3, 4]. Many different analyses by the IceCube Collaboration have confirmed independently the existence of such a signal, even though, so far, its possible sources are still barely accessible. Some tension is present in the observed cosmic flux as discussed in [5]. A local source for at least part of the overall diffuse flux seems necessary in most models.

A sophisticated way to address the issue has been proposed recently [6]. A toy-model for the local galactic environment has been used to study the behaviour of Cosmic Rays in the proximity of the Solar system. Cosmic rays produced and accelerated by a young and efficient accelerator, such as a Supernova remnant close to our Solar System, would behave differently in our proximity with respect to what would result from homogeneous propagation in the Galaxy. Indeed, our local neighbourhood is characterised by the Local Hot Bubble, in which the Solar System is located, and the Superbubble induced by stellar activity in the Cen-Sco association, the association of OB stars closest to our Solar System, located about 300-400 pc away. The intersection between the two bubbles allegedly produces the Loop1 radio feature. Being this interface close to the Earth (50-100 pc away) it covers a large part of the radio sky, showing up as a 60 degree-radius (almost) circular structure. An artistic depiction of the local galactic environment is reported in figure 1.

Inhomogeneities in matter density and magnetic fields produced by the crossing of the two bubbles can modify the behaviour of Cosmic Rays in our local environment with respect to the average observations through the Galaxy. This could then in turn produce particular features in the Cosmic Rays spectrum and the subsequent neutrino signal. In particular, the toy model discussed there would produce an enhancement of the neutrino rate in the few-tens-of-TeV energy range, analogous to that observed in IceCube all-sky analyses. If this enhancement happens at the interface between the two bubbles, it might appear as a largely extended neutrino emitting region in the ANTARES sky.

2. Neutrinos from local superbubbles

Massive stars lose a significant fraction of their mass by stellar winds. As this wind expands, a low-density bubble is created in the interstellar medium. Similarly, at the death of the star, its explosion as a core-collapse supernova injects a shock-wave into the interstellar medium, causing further perturbation in the bubble. The same processes modify the behaviour of the local magnetic fields, enhancing them at the boundary of the bubble (the “wall”). Since massive stars are formed in clusters, the wind-blown bubbles of individual stars encounter each other as they expand and merge to form a single superbubble. Its shape is determined by the pre-existing density inhomogeneities and magnetic fields, as well as the positions of the first Supernovae.



Figure 1: Artist's conception of the Local Bubble (containing the Sun and Beta Canis Majoris) and the Loop1 Bubble (containing the star Antares). The interface between the two Bubbles produces the Loop1 feature.

Since this geometry can be very complicated, an idealised superbubble is considered in [6] so that a computational model of this environment can be defined. In this toy-model, the magnetic field and density profiles are perpendicular to the Galactic plane, and show a cylindrical symmetry. The magnetic field strength inside the bubble is set to $0.1 \mu G$, to $12 \mu G$ in the wall and $5 \mu G$ outside. The regular magnetic field outside the bubble in the Galactic disc is assumed to be constant and pointing in one direction, i.e. the curvature of the spiral arms is ignored. The bubble is given a 50 pc radius, with a 2 pc-thick surface layer. Cosmic rays are injected, propagated and tracked in this simplified environment; their flux and that of their interaction products is recorded. Different injection assumptions are considered, ranging from a continuous/steady source to a bursting one. When the Cosmic Ray source is given the properties of the Vela SNR, and the cosmic radiation is considered for the Sun location in the bubble, the spectra shown in figure 3 of [6] are obtained. In particular, the all-flavour neutrino spectrum due to the effects of Cosmic Rays propagating in the Solar neighbourhood described there can be fitted as as:

$$E_\nu^2 \times \Phi_{local} = 16/6 \times 10^{-9} \left(\frac{E_\nu}{1 \text{ TeV}} \right)^{0.78} \times \left(\frac{1 + E_\nu}{10 \text{ TeV}} \right)^{-0.75} \times \left(\frac{1 + E_\nu}{150 \text{ TeV}} \right)^{-1.67} \times e^{-E_\nu/2 \text{ PeV}} [\text{GeV cm}^{-2} \text{ s}^{-1} \text{ sr}^{-1}] \quad (2.1)$$

Being the Sun close to the Local Hot Bubble wall and to the interface between the two bubbles, this interface would produce remarkable effects over different wavelengths. Because of proximity, it would be observed as an extremely extended feature of the sky. This is the case in all-sky radio

observation, where a 60° -radius structure, centred at galactic coordinates $(-30^\circ, 17^\circ)$, is visible. So-called “loops” and “filaments” are common features of the radio sky, Loop1 being the most prominent and the largest one.

The authors of [7], analysing microwave data from WMAP, have found that non-thermal dust emission (e.g. from magnetic dipole from dust grains, arising from thermal fluctuations in the magnetization of grain materials) is present in the CMB residuals when considering an annular structure superimposed to Loop1. Though the significance of this observation is limited (p -value = 0.01), it could be hinting to magnetic and matter inhomogeneities at the borders of the Loop1 interface surface as expected in the toy-model described above.

The Planck collaboration has dedicated large space to the analysis of Galactic foregrounds, studying both intensity and polarisation at the different wavelength accessible with both Planck and WMAP data. In particular, Loop1 is analysed in detail in section 5 of [8] by means of a multi-wavelength analysis of this emission regions. Loop1, as a 60° -radius (complex) structure, is clearly observable in polarisation maps from the combination of the Planck and WMAP data-sets. In particular, at the highest frequency, the emission can be modeled using a synchrotron hypothesis, properly reproducing the polarisation features in Planck data.

Multi-wavelength observations of the Loop1 region extend up to very-high energies. In particular, the largest feature of the diffuse ROSAT X-ray observations (and in particular in the $\frac{3}{4}$ keV energy band) follows the same shape as Loop1. The X-ray emission shows a strong resemblance with the main features of the Loop1 observation at lower energies. In particular, the brightest section of this emission is the so-called “North Polar Spur” (NPS), a large arc extending above the Galactic Plane. Most of the models attribute this feature to the hot interstellar bubble from the Cen-Sco association, and in particular with the remnant of a SuperNova in the proximity of the wall of the superbubble, as suggested by [9]. However, both the Planck Loop1 analysis and a specific analysis using detailed measurements with XMM-Newton in X-rays coming from the direction of the NPS [10] and infrared studies of the possible matter density in CO-H₂ seem to point to a distance of the NPS to Earth larger than 300 pc (being of the order of 1 kpc) and thus not compatible with it being part of the bubble interface from which signal neutrinos are searched for here.

3. Searches for cosmic neutrinos in ANTARES

The ANTARES underwater neutrino telescope [11] is located 40 km off-shore Toulon, France, in the Mediterranean Sea ($42^\circ 48' N$, $6^\circ 10' E$). It consists of a three-dimensional array of 885 10-inch photomultiplier tubes (PMTs) distributed along 12, 450 m long, vertical lines, anchored to the sea-bed at a depth of about 2500 m and kept taut by top buoys.

Relativistic charged particles moving in the proximity of the detector produce Cherenkov photons. The passage of these particles can produce detectable signal on the PMTs. The position, time and collected charge of these signal (“hits”) are exploited by reconstruction algorithms in order to estimate the direction and energy of the particle. Triggers, based on combinations of space-time coincidence between hits, are applied to discard events produced by environmental light emitters like inorganic ^{40}K decays and organic bioluminescence [12]. All data collected by the PMTs are transferred to shore, where this data reduction process is done. The varying conditions of the data-acquisitions and detector setup are simulated by means of Monte Carlo simulation [13].

Charged Current (CC) interactions of muon neutrinos produce a track signature in the detector. For these events, a median angular resolution as low as 0.4° is achieved [14]. All-flavor Neutral Current (NC) as well as ν_e and ν_τ CC interactions produce electromagnetic and hadronic showers with an almost point-like emission of Cherenkov photons. These events are reconstructed when the neutrino interacts close to, or inside, the instrumented volume [15] with a median angular resolution of the order of 3° and a relative energy resolution as low as 10% in the case of CC ν_e interactions above some tens of TeV.

Even though the detector is optimised so that it can search for neutrino-induced events, most of the physical signals collected with the apparatus are due to penetrating muons coming from cosmic ray showers in the atmosphere. However, only neutrinos can actually traverse the Earth, thanks to their small interaction cross section with matter, and the whole Earth can be used as a shield against atmospheric muons, by selecting only at upward-going particles. The residual contribution of atmospheric muons that are wrongly-reconstructed as upward-going particles is usually reduced by means of an event selection based on the quality parameters produced by the reconstruction algorithms. After a proper reduction of the atmospheric muon contribution, a sample of neutrino-induced events survives. Atmospheric neutrinos are topologically indistinguishable, in the case of the ANTARES detector, from cosmic neutrinos. The most remarkable difference between background and signal neutrinos is indeed given by their energy spectrum. An energy reconstruction-related selection allows a statistical separation between the signal and the backgrounds. More details on the atmospheric backgrounds are given in ref. [5].

3.1 Event selection optimisation

In order to properly define an optimal event selection for the rejection of atmospheric events maximising the sensitivity of the experiment, a Model Rejection Factor [16] minimization procedure is applied to obtain the best selection cut.

Let $\Phi(E)$ be the theoretical source flux, n_s the number of expected signal events, n_b the expected background and n_{obs} the number of events observed in a hypothetical experiment. If the number of observed events is compatible with the background, the upper limit for the flux at 90% confidence level (C.L.) is:

$$\Phi(E)_{90\%} = \Phi(E) \frac{\mu_{90}(n_{obs}, n_b)}{n_s}, \quad (3.1)$$

where $\mu_{90}(n_{obs}, n_b)$ is the Feldman-Cousins upper limit [17].

The ‘‘average upper limit’’ that would be observed by an ensemble of hypothetical experiments with no true signal ($n_s = 0$) and expected background n_b can be computed. Taking into account all the possible fluctuations for the estimated background, weighted according to their Poisson probability of occurrence, the average upper limit is:

$$\bar{\mu}_{90}(n_b) = \sum_{n_{obs}=0}^{\infty} \mu_{90}(n_{obs}, n_b) \frac{n_b^{n_{obs}}}{n_{obs}!} e^{-n_b}. \quad (3.2)$$

The best upper limit is obtained with the best cut that minimises the Model Rejection Factor (MRF):

$$MRF = \frac{\bar{\mu}_{90}}{n_s} \quad (3.3)$$

and hence minimises the average upper limit flux

$$\bar{\Phi}(E)_{90\%} = \Phi(E) \frac{\bar{\mu}_{90}}{n_s} \quad (3.4)$$

or, equivalently, provides an estimate of the best sensitivity of the experiment.

The ANTARES track sample described in [18] has been used in this analysis, covering a total of about 3200 days of data-taking time. The ANTARES sensitivity can be estimated assuming that the entirety of the flux described by equation 2.1 comes from either one of the two following options:

1. a disk, centred at galactic coordinates $(-30^\circ, 17^\circ)$ with a radius equal to 60° , covering π sr;
2. a ring, centred at galactic coordinates $(-30^\circ, 17^\circ)$ with an external radius equal to 60° and an inner radius equal to 50° , covering 0.96 sr.

Restricting the observation to a smaller region of the sky automatically reduces the amount of background events and, once the signal flux is kept constant, improves the signal to noise ratio. The ring-shaped emission will be considered here in the results.

An extra-galactic background is considered, according to the best-fit of the IceCube signal flux from the Northern sky, fitted by an $E^{-2.1}$ unbroken single-power-law energy spectrum. Indeed, as explained in [6], the all-sky neutrino flux observed in data collected by the IceCube Neutrino Observatory can be explained in terms of this extra-galactic component on top of which a low-energy flux is produced by these local effects coming from cosmic ray interactions in local superbubbles. The effect of this background is relatively small and does not influence significantly the event selection choice; this has been tested adding also an high-energy cut in the event selection so that it could exclude the high-energy tail of the background, but this cut would not affect the resulting sensitivity.

4. Results and outlook

Figure 2 shows the sensitivity of ANTARES in the track channel for a ring-shaped neutrino emission according to the flux of equation 2.1, compared to the models for the local emission from the bubble and the extragalactic neutrino spectrum. The sensitivity flux is about 3.6 times larger than the model signal flux for the emission region. The sensitivity range is defined as the energy range where the central 90% of signal events is expected after the energy selection, and goes from 11 to 200 TeV.

Once data from the on-zone are compared to the observation in the off-zone, 22 events are observed in the signal region, while 18 events are present in the background one. This corresponds to a 0.9σ excess according to the Li&Ma method [19]. The corresponding 90% confidence level upper limit is shown in figure 2. The limit is worse than the sensitivity – 6.5 times larger than the reference flux from the model, while the sensitivity is a factor 3.6 above the model – since an overfluctuation with respect to the background expectations is observed.

The sensitivity of ANTARES can be improved by including shower-like events. In this case, the expected background should be smaller than in the case of track-like events since the atmospheric neutrino flux is less intense. However, the ANTARES effective area for this event topology

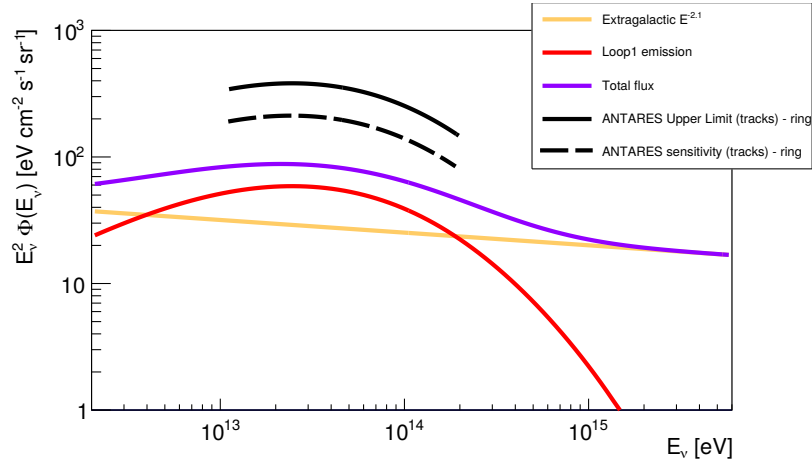


Figure 2: ANTARES (2007 - 2017 data-set) 90% confidence level upper limit (black line) in the track channel to a neutrino emission following the spectrum described in equation 2.1 under the assumption that the flux comes from ring region described in the text, in terms of contributions to the all-sky neutrino diffuse emission. The upper limit is compared to the predictions from [6], depicted as a red line, and the extragalactic contribution observed in the IceCube North sample (red line); the sum of the two is overall cosmic flux shown as a purple line. The sensitivity flux is shown as a dashed line. Fluxes are shown as three-flavour fluxes, in the assumption of equipartition between the three neutrino flavours.

is also smaller, due to the fact that only events within a fiducial volume are taken into account for the analysis. All things considered, the contribution to the sensitivity coming from shower-like events has been estimated of the order of 30% in searches for point-like emissions where the worse angular resolution for shower-like events with respect to track-like events worsen the impact of shower-like events. This factor is mildened when looking at extended regions of the sky, such as the parts of the sky analysed in this work. The inclusion of shower-like events in this analysis is currently in progress.

Acknowledgements

This project has received funding from the European Union’s Horizon2020 research and innovation programme under grant agreement N° 739560 (KM3NeT 2.0)

References

- [1] R. Coniglione, on behalf of the ANTARES and KM3NeT Collaborations, PoS(ICRC2019)006
- [2] M. G. Aartsen et al., *Physical Review D* **91** (2015) 022001
- [3] M. G. Aartsen et al., *Astrophysical Journal* **809** (2015) 98
- [4] M. G. Aartsen et al., *Astrophysical Journal* **833** (2016) 3
- [5] L.A. Fusco and F. Versari, on behalf of the ANTARES Collaboration, PoS(ICRC2019)891
- [6] K.J. Andersen, M. Kachelriess and D.V. Semikoz, *Astrophysical Journal Letters* **861** (2018) L19
- [7] H. Liu, P. Mertsch and S. Sakar, *Astrophysical Journal Letters* **789** (2014) L29

- [8] The Planck Collaboration, *Astronomy & Astrophysics* **594** (2016) A25
- [9] M. Wolleben, *Astrophysical Journal* **664** (2007) 349-356
- [10] R. Lallement et al., *Astronomy & Astrophysics* **595** (2016) A131
- [11] M. Ageron et al., *Nucl. Instrum. Meth. A* **656** (2011) 11
- [12] J.A. Aguilar et al., *Nucl. Instr. and Meth. A* **570** 1 (2007) 107 (2007)
- [13] L.A. Fusco and A. Margiotta, on behalf of the ANTARES Collaboration, *EPJ Web Conf.* **116** (2016) 02002
- [14] S. Adrián-Martínez et al., *Astrophys. J.* **786** (2014) L5
- [15] A. Albert et al., *The Astronomical Journal*, **154** (2017) 275
- [16] G.C. Hill and K. Rawlins, *Astroparticle Physics*. **19** (2003) 393
- [17] G.J. Feldman and R.D. Cousins, *Physics Review D* **57** (1998) 3873
- [18] A. Albert et al., *Astrophysical Journal Letters* **863** (2018) L30
- [19] T.P. Li and Y.Q. Ma, *Astrophysical Journal* **272** (1983) 317